

Influence of gaps' geometry change on leakage flow in axial piston pumps

Piotr Patrosz1[0000-0002-8711-7062]

¹Gdansk University of technology, ul. Narutowicza 11/12, Gdansk 80-233, Poland

piotr.patrosz@pg.edu.pl

Abstract. Axial piston pumps are the core elements of most medium and high-pressure hydraulic systems. High volumetric efficiency and high working pressures are the main advantages of this type of pumps. Therefore it is necessary to accurately calculate the leakage flow through the gaps to design efficient high-pressure pump. The main difficulty of such calculations is the fact, that the gaps change their geometry during pumping process. The change of gaps' geometry can be caused by the motion of pump's elements or can be pressure-induced. Both of these factors are included in the article. The paper describes the leakage in: gap between piston and cylinder block, gap in commutation window, gaps in hydrostatic bearings, gap between commutation plate and cylinder block. The article includes methodology and results of FEM and CFD simulation of flow through deformed and undeformed gaps. Basing on the CFD results the mathematical models of such gaps were prepared and added to the article.

Keywords: Hydraulics, Pumps, CFD.

1 Introduction

Axial piston pumps are the core elements of most medium and high-pressure hydraulic systems. Thanks to their high volumetric efficiency, high working pressure and potential to work as variable displacement machines they are considered one of the most versatile hydraulic pumps. They are the only type of pumps that are used in closed loop circuits and dominated the market of variable displacement pumps used in medium and high-pressure open circuits. Thanks to this features the engineers are facing a hard challenge to develop new, even more efficient pumps, that can beat the competition. To increase the efficiency of the piston pumps it is necessary to lower the leakage flow rate through the gaps. The problems of gap flow is well described in the literature [1]. However most of the mathematical models are stationary and does not include the change of gap geometry caused by the motion of pump elements or by deformation of these elements.

1.1 Design of axial piston pumps

To fully understand how these gaps are changing it is necessary to shortly describe two types of axial piston pumps that are the subject of the article. First is the axial piston pump with plate commutation (Fig. 1) and the second is axial piston pump with cam driven commutation (Fig. 2), which is designed and developed at Gdansk University of Technology [2]. The first type is the most common. It consists of a shaft 1 that is combined with rotary cylinder block 3. Pistons 4 are rotating with cylinder block and are cooperating with stationary, slanted swash plate 7 using slippers 6. The reciprocating movement of pistons cause the pumping and sucking of the fluid. The commutation plate 5 (Fig. 1b) is responsible for connecting right channels during pumping and sucking process, in order to ensure, that the fluid is pumped out of the high-pressure outlet P and sucked through the low-pressure inlet S (Fig. 1c). During the switching process working chamber may be disconnected from both P and S channels, what will depending how this channels overlay or not the channel in the cylinder block during the switching process.

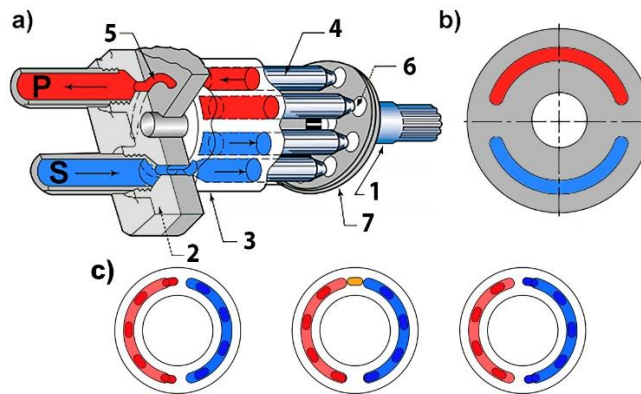


Fig. 1. Axial piston pump with plate commutation [3]: a) cross section of the pump; b) commutation plate c) basics of operation of commutation unit (1 – shaft; 2 – casing; 3 – cylinder block; 4 – piston; 5 – commutation plate; 6 – slipper; 7 – swash plate; P – outlet; S – inlet; red color – high pressure; blue color – low pressure, yellow color – disconnected channel to the working chamber)

The second type of the axial piston pump that is taken into consideration is the PWK axial piston pump with cam driven commutation (Fig. 2). The main difference of this pump is that there are two groups of pistons 4 placed inside a stationary cylinder block that is a part of a casing 2. The pistons movement is generated by the rotating swash plates 7 connected with shaft 1. Such configuration makes it impossible to use plate commutation. Therefore cam driven commutation mechanism was used. This mechanism consists of commutation tubes 9 cooperating with cam 11 through plastic slippers 10. The cam 11 is rotating with the shaft 1. Its movement pushes the commutation tubes 9, so that the commutation window can connect a working chamber with P channel

during pumping process and S channel during suction. The pump enables the displacement change by changing cam 11 position relative to the shaft 1. The displacement change is obtained thanks to the mechanism consisting of a stepper motor 14, planetary gear 13 and connecting shaft 12. In case of the pump with cam driven commutation the displacement change does not directly affect the value of the leakage flow rate, because the angle of the swash plate remains constant. The displacement impacts indirectly the leakage flowrate only during short time, when the working chamber is cut off by the commutation. Although this phenomenon is very important when calculating pressure peaks[4], due to its short time of occurrence it can be treated as negligible in overall leakage calculations. In case of pumps with plate commutation the displacement change affects the leakage flowrate, because the angle of the swash plate changes and this affects values of forces working on the pistons what is included further in the article.

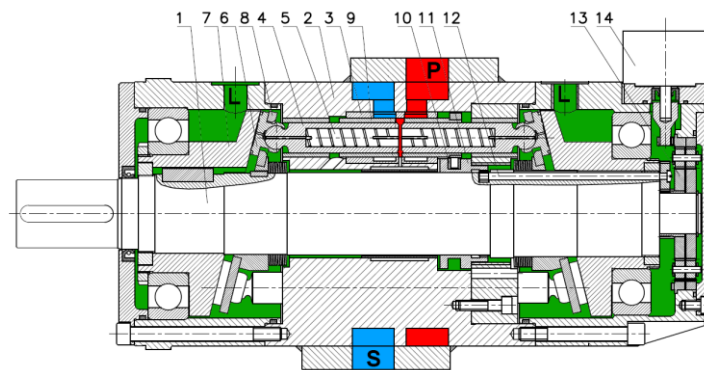


Fig. 2. PWK axial piston pump with cam driven commutation (1 – shaft; 2 – casing; 3 – bronze sleeve; 4 – piston; 5 – spiral choke; 6 – slipper; 7 – swash plate; 8 – separator plate; 9 – commutation sleeve; 10 – plastic slipper; 11 – cam; 12 – connecting shaft; 13 – planetary gear; 14 – stepper motor; P – outlet; S – inlet; red color – high pressure; blue color – low pressure, green color – casing pressure)[3]

1.2 Main leakage sources in axial piston pumps

In both described types of axial piston pumps the sources of leakage (Fig. 3 and 4) are similar:

- leakage through an annular gap between the piston and cylinder block (Fig. 3 and 4 purple color),
- leakage through a hydrostatic bearing under a slipper (Fig. 3 and 4, red color),
- leakage through a gap in commutation (Fig. 3 and 4, green color).

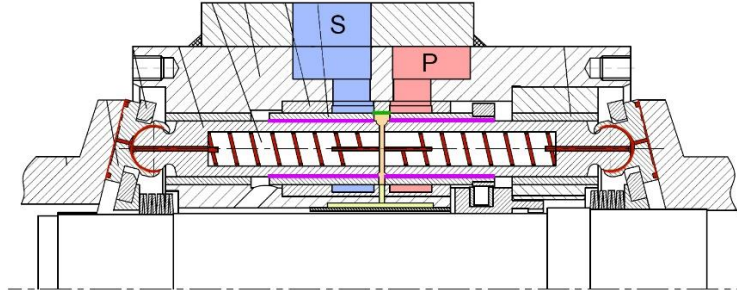


Fig. 3. Leakage sources in PWK axial piston pump with cam driven commutation (red – leakage through a hydrostatic bearing under a slipper; green – leakage through a commutation window; purple – leakage through an annular gap around piston; light blue – low pressure, pink – high pressure)[4]

Only in case of a pump with plate commutation, there will be an additional leakage source through a hydrostatic bearing under a cylinder block (Fig 4, orange color).

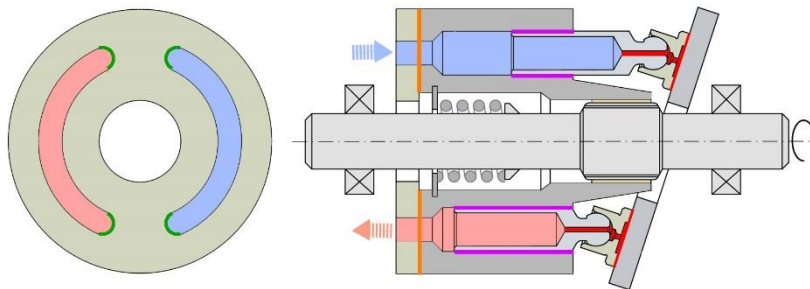


Fig. 4. Leakage sources in axial piston pump with plate commutation (red – leakage through a hydrostatic bearing under a slipper; green – leakage through a commutation window; purple – leakage through an annular gap around piston; orange – leakage through a hydrostatic bearing under cylinder block; light blue – low pressure, pink – high pressure) [5]

Almost every mentioned above gap change its shape when the pump is working. This change can be a result of a movement of elements or may be caused by pressure growth. Additionally thermal deformations are also possible, however they will not be taken into consideration in this article, but the interested reader will be able to find lots of information about them in the literature [6, 7]

2 Models of leakage flow rate in gaps

Since the internal leakage of the pump is hard to measure, and distinguishing its source is even harder, CFD and mathematical models were prepared. Their main task is to predict the value of leakage flow rate through each gap.

2.1 Annular gap around piston

Definition of the flow rate through an annular gap around piston is very much similar in both types of axial piston pumps. It has been described in [1,12,13,14,15] The simplified sketches of the possible gap geometries are presented in Fig. 5. The annular gap can be coaxial, eccentric or skewed, however fast moving piston has tendency to position itself parallel to the cylinder. Therefore eccentric gap will be taken into further consideration. If the gap is considered non-deformable and the flow is assumed laminar, the equation defining the flow rate can be noted as [1]:

$$Q_A = \frac{\pi \cdot \Delta p_A \cdot d_t \cdot h_A^3}{12 \cdot \nu \cdot \rho \cdot L_t} (1 + 1.5(\varepsilon)^2) \quad (1)$$

where:

Δp_A – pressure drop between the inlet and the outlet of the annular gap,

d_t – diameter of the annular gap,

h_A – annular gap height,

L_t – annular gap length,

ν – fluid's kinematic viscosity,

ρ – fluid's density,

$\varepsilon = e/h_A$ – eccentricity of the piston,

e – eccentric displacement.

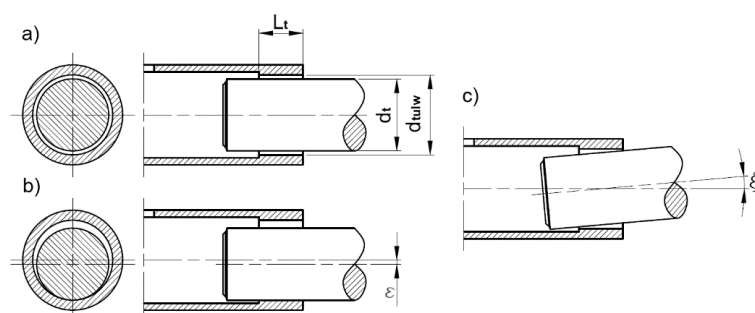


Fig. 5. Annular gap: a) coaxial; b) eccentric; c) skewed [4]

The equation (1) can be considered as correct for pumps with plate commutation, since the pistons are fitted directly into virtually thick and rigid cylinder block. Pistons in pumps with cam driven commutation are fitted in relatively elastic commutation sleeves which can be deformed by pressure. Using Lamé's equation (2) [8] to determine radial deformation Δr , of a sleeve and eq. (1), eq. (3) was derived[4].

$$\Delta r = \Delta p_A \left\{ \frac{d_{tulw}^2}{2E(d_{tulz}^2 - d_{tulw}^2)} \left[(1 - \nu)d_{tulw} + (1 + \nu) \frac{d_{tulz}^2}{d_{tulw}} \right] \right\} = \Delta p_A \cdot A \quad (2)$$

$$Q_{Adef} = \frac{\pi \cdot d_t}{12 \cdot \nu \cdot \rho \cdot L_t} \left(\frac{\Delta p_A^4 \cdot A^3 + 4h_A \cdot \Delta p_A^3 \cdot A^2 + 6h_A^2 \cdot \Delta p_A^2 \cdot A + 4h_A^3 \cdot \Delta p_A}{4} + 1.5\varepsilon^2 \cdot h_A \cdot \Delta p_A + 0.75A \cdot \Delta p_A^2 \varepsilon^2 \right) \quad (3)$$

where:

E – Young modulus,

d_{tulz} – external diameter of a sleeve,

d_{tulw} – internal diameter of a sleeve,

ν – Poisson's ration.

Using the eq. (3) it is possible to calculate the flow rate through the deformable annular eccentric gap. It includes the fact that the pressure at the inlet of the gap is much higher than in the outlet. Therefore the gap height will be greater on the inlet side then on the outlet.

2.2 Slipper-swash plate gap

One of the most important gaps in every piston pump is the gap between slipper and swash plate. The leakage through this gap is necessary for supporting hydrostatic bearing between cooperating elements. The created gap is a radial gap limited by diameters d_{phsw} and d_{phsz} (Fig. 6).

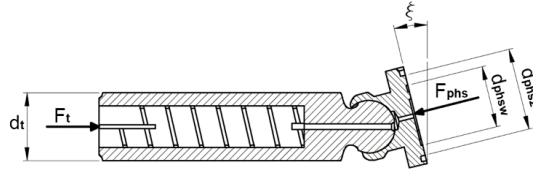


Fig. 6. Sketch of the piston and slipper[4]

To calculate the flow through it, the pressure p_{phs} in the hydrostatic bearing has to be determined. Using the force equilibrium:

$$F_t = F_{phs} \cos \xi, \quad (4)$$

eq.(5), is derived:

$$p_{phs} = (p_p - p_c) \cdot \frac{2 \cdot d_t^2 \cdot \ln\left(\frac{d_{phsz}}{d_{phsw}}\right)}{d_{phsz}^2 - d_{phsw}^2} \cos \xi \quad (5)$$

where p_p is pumping pressure and p_c is the casing pressure.

Flow rate through the radial gap, if this gap is nondeformable might be calculated using the equation:

$$Q_{phs} = \frac{\pi \cdot p_{phs} \cdot h_{phs}^3}{6 \cdot \nu \cdot \rho \cdot \ln\left(\frac{d_{phsz}}{d_{phsw}}\right)} \quad (6)$$

Unfortunately gap height h_{phs} is hard to determine. Therefore the eq. (6) is difficult to use without numerical methods. To overcome that problem the flow can be indirectly calculated using eq. (7)[9] defining the flow in spiral choke (Fig.7):

$$Q_{phs} = k_{dl} \frac{(p_p - p_{ph}) \cdot h_{dl}^4}{\nu \cdot \rho \cdot L_{dl}} \quad (7)$$

where:

k_{dl} – geometry coefficient,

L_{dl} – length of a spiral.

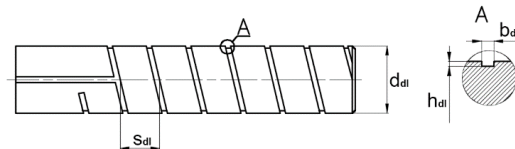


Fig. 7. Sketch of a spiral choke[4]

k_{dl} coefficient is obtained from CFD simulation equals 0,087. Finite element model used to compute k_{dl} coefficient was prepared (Fig. 8). It consisted of 400 000 hexahedral elements, didn't include heat transfer and was calculated in ANSYS CFX using SSQ turbulence model. The inlet and outlet boundary conditions were applied on the opposing ends of the spiral choke. To the rest of the model walls, the no-slip wall boundary condition was applied. CFD model proved to be accurate comparing to the results of measurements presented in [9].

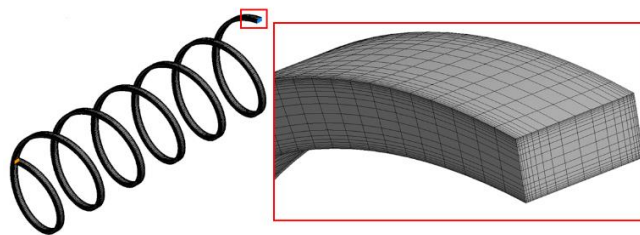


Fig. 8. Model of a spiral choke used in CFD calculations

Since the method of calculating the flow in slipper-swash plate gap is indirect, it is not highly sensitive to the gaps height variation. To assess how the deformation of the gap, caused by pressure, can impact gap height, resulting in change of pressure distribution, the FEM calculations were conducted. Slipper FEM model (Fig.9) consisting of 38945 mainly hexahedral finite elements and loaded with pressure gradient with

maximal value of 25MPa applied to the slipper pocket. This pressure will appear in hydrostatic bearing when the pumping pressure is $p_p=30\text{MPa}$. The slipper is supported using frictionless support marked as blue region in Fig. 9a, and by elastic support marked as yellow region. This support was very elastic and didn't affect the solution, but stabilized the solver. Considering these boundary conditions the height of radial gap may increase locally only by $0,6\mu\text{m}$. This will not influence the pressure distribution significantly. Therefore the influence of the deformation, caused by the pressure can be treated as negligible when using eq.(7).

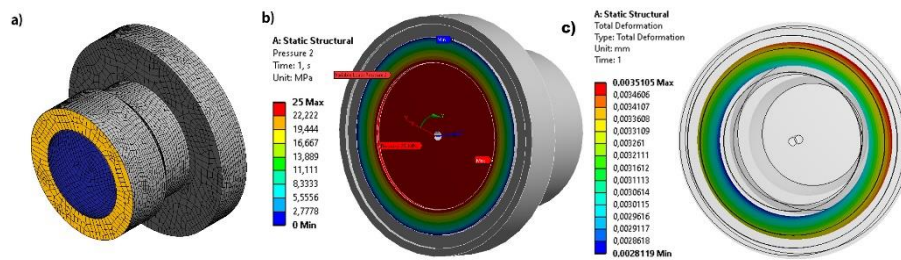


Fig. 9. Slipper deformation FEM model and results: a) mesh and supports, b) load pressure gradient, c) deformation of the gap

The elastohydrodynamic lubrication effects also should be taken into consideration, because the motion of the fluid film, caused by pistons or swashplate rotation, can change the pressure gradient under the slipper, positioning the slipper under slight angle to the swash plate. This phenomenon would be very important when calculating the flow rate directly through a slipper using eq. (6). However assuming that the hydrostatic pressure in a pocket under the slipper is relatively high and its changes, even considering the EHL effects, are not significant, the indirect calculations of the flow through a choke in a piston, would give good results with reasonably low error, maintaining relatively simple mathematical notation (7), in comparison with direct calculations which will have to include FSI numerical solution to obtain accurate results.

For pumps with different chokes inside the pistons, equations (4) and (5) are still applicable, however eq. (7) has to be replaced with the other equation corresponding with the right choke type.

2.3 Commutation gap

Commutation gap is a gap that is created between the commutation window and inlet or outlet channels. The flow through this gap is very specific for every pump. It strongly depends on the shape of commutation window and on the position of cylinder block or commutation sleeve. Additionally this gap rapidly changes its length and is only opened for a short time when the commutation window is in a position between inlet and outlet channels. Commutation gap is a dynamic and complex gap. Flow through this gap cannot be accurately calculated without doing experimental measurements or

using CFD tools. Therefore in this article the commutation gap leakage flow rate calculation is shown on an example of a pump with cam driven commutation. The simulations were conducted for the commutation window in the commutation sleeve. The model used for simulation is presented in Fig. 10.

The CFD model included: commutation window inside the sleeve, low pressure channel and annular gap between them. In the model the window is moving away from the channel so that the flow between them occurs only through the annular gap. The results of simulation are shown in Fig. 11.

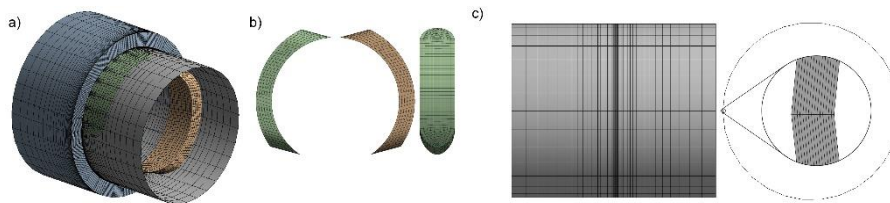


Fig. 10. Model of gap in commutation window: a) full model, b) model of the window, c) annular gap

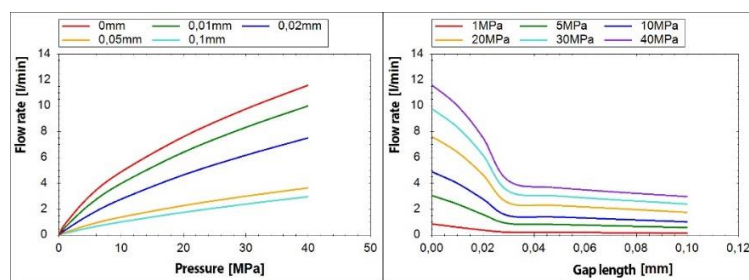


Fig. 11. Flow rate through the commutation gap in function of pressure and gap length calculated using the CFD model presented in Fig. 10 [4]

Sketch of the gap used for further analytical calculations is presented in Fig. 12.

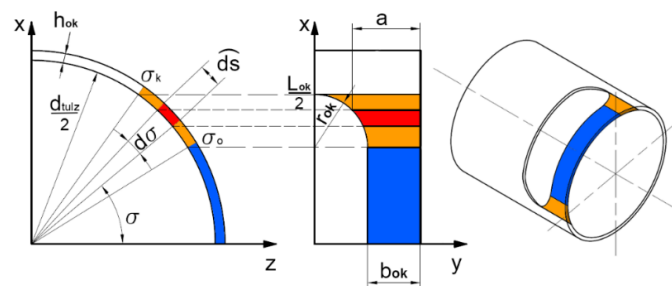


Fig. 12. Sketch of the commutation gap

Mathematical model of the commutation gap (Fig. 12) is defined with the equation[4]:

$$Q_{ok} = Q_{lam} \cdot f(b_{ok}) + Q_{tur} \cdot (1 - f(b_{ok})) \quad (8)$$

where:

$f(b_{ok})$ is the transition function given by empirically specified logistic function[4] :

$$f(b_{ok}) = \frac{1}{1 + e^{-18\left(\frac{b_{ok}}{5[mm]} + 1\right)}} \quad (9)$$

Q_{lam} is the laminar component of the flow and is given by the equation[4]:

$$Q_{lam} = \frac{(p_p - p_c) \cdot d_{tulz} \cdot h_{ok}^3}{12 \cdot \nu \cdot \rho} \left[\frac{\sigma_o}{b_{ok}} + \int_{\sigma_o}^{\sigma_k} \frac{d\sigma}{b_{ok} + r_{ok} - \sqrt{r_{ok}^2 - \left(\frac{d_{tulz}}{2} \sin \sigma - \frac{L_{ok} + r_{ok}}{2}\right)^2}} \right] \quad (10)$$

Q_{tur} is the laminar component of the flow and is given by the equation[4]:

$$Q_{tur} = h_{ok} \cdot L_{ok} \sqrt{\frac{2(p_p - p_c)}{\zeta_{ok} \cdot \rho}} \quad (11)$$

where ζ_{ok} is the empirical flow resistance coefficient.

2.4 Cylinder block commutation plate gap

The last and the most complex gap is the gap between cylinder block and the commutation plate. The fluid film in this gap provides a hydrostatic bearing which supports rotating cylinder block, which is pushed towards the stationary commutation plate by the forces from pistons and pressures inside the working chambers. The distribution of the pressure in the gap is presented in Fig. 13a[11]. This pressure gradient constantly changes, depending on the position of the cylinder block. This gradient should cancel the forces mentioned earlier, but because of the fact that number of pressurized working chamber is constantly changing (Fig. 1c), and because of a geometric features of the cylinder block and the commutation plate, value and position of the gradient isn't ideal, what causes the gap to be skewed, as its shown in Fig. 13b.

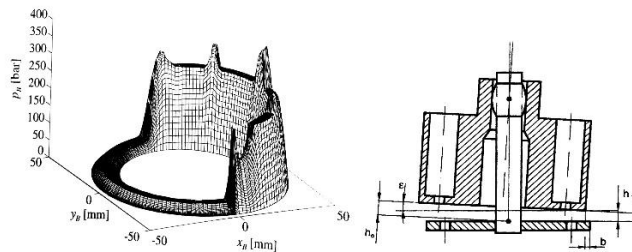


Fig. 13. Gap between cylinder block and commutation plate a) pressure distribution in the gap [11] b) gap shape [2]

Additionally the flow in the commutation gap doesn't occur only to the casing of the pump but it also occurs between the channels in the commutation plate, therefore the flow rate through gap depends on an angular position of the cylinder block (Fig. 1c) and the overlap of commutation window, which will determine for how long the working chamber may remain cut off from both channels in the commutation plate. This may lead to a sudden change of pressure in the working chamber and cause an appearance of unbalanced forces in the hydrostatic bearing which may lead to a temporary leakage flowrate change.

The only accurate method of determining the flow rate through this gap is the CFD and structural FEM analysis. Unfortunately, description of this method exceeds the capacity of that article. Therefore it is recommended for the interested reader to check the articles [10, 11] and especially a book [2] from, which some of the results are presented in next chapter.

3 Results and discussion

Using the equations from the previous chapter Fig. 14-17 were created. Fig. 14 presents the comparison of the flow through a deformable annular eccentric gap between. As it is presented the influence of gap deformation is considerable, therefore omitting this phenomenon is not recommended especially in pumps with cam driven commutation. Such big difference is caused by the fact, that in eq. (3) gap height is in third power. Therefore, if height of the undeformed gap is about $10\mu\text{m}$ and the radial deformation can exceed $5\mu\text{m}$, the flow rate through the gap can increase over 3.3 times.

Flow rate through the gap between a single slipper and swash is presented in Fig. 16. The chart presents difference between the results of CFD simulations (red) and results of calculations using eq. (7). As it is visible the chart obtained from simulations is a little nonlinear, which indicates that the flow is not fully laminar. However the analytical model (7) assumes the laminar flow. The difference between the simulation and calculations is small and for most needs can be treated as negligible.

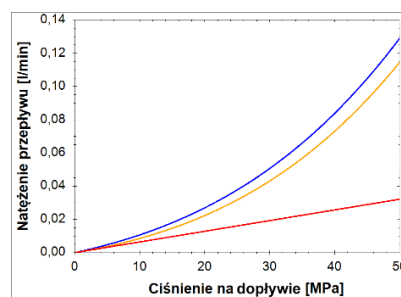


Fig. 14. Flow rate through the annular gap between the piston and cylinder [4]: red - nondeformable central gap; yellow – deformable central gap, blue – deformable eccentric gap

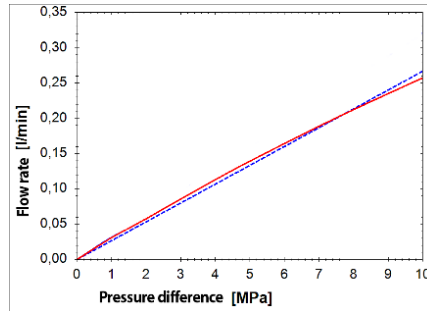


Fig. 15. Flow rate through the spiral choke and slipper-swashplate radial gap: red – simulation result, blue – result of calculations using eq. 7 [4]

The flow rate through the gap in commutation window is presented in a Fig. 17. On the chart the analytical and CFD models are compared. Compatibility of the results is between 80-90%, what in most cases can be assumed as good convergence, especially taking into account the fact, that the gap is opened only for a short period, when the commutation window is between the inlet and outlet channel. For the rest of a time, when the length of the gap exceeds 1mm the flow rate through it is negligible.

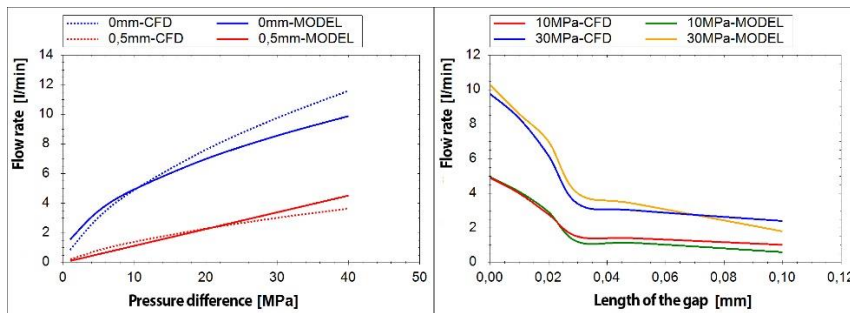


Fig. 16. Flow rate through the commutation gap

The flow rate Q through the gap between the cylinder block and commutation plate is supposed to be responsible for 30-50% [10] of volumetric losses in piston pumps. Additionally it is highly dependable on angular position φ of the cylinder block. Unfortunately all the simulation in the literature [2, 10] does not separate the flow through this gap to the casing and between the channels in the commutation plate. The example of this results are shown in Fig. 17.

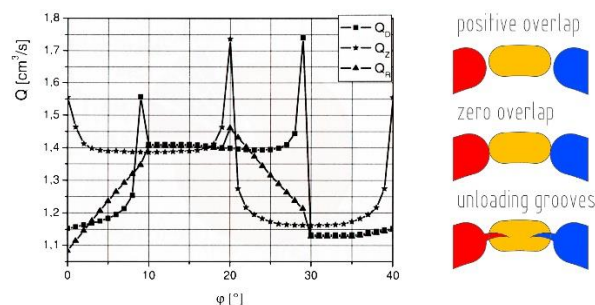


Fig. 17. Leakage flow rate through a gap between the cylinder block and the commutation plate [2]: Q_D – positive overlap; Q_Z – zero overlap; Q_R – unloading grooves

The presented in Fig. 17 results of CFD simulation show also the influence of the overlap and usage of unloading grooves on the flow rate. Fig. 17 presents that when zero or positive overlap is used, the significant flowrate spikes can be observed. As it was written before the unbalanced forces working on the cylinder block cause the deformation of the gap and as a consequence sudden flowrate change. Usage of the unloading grooves in the presented model decreased the flowrate spikes and overall leakage comparing to positive overlap. The model used to prepare Fig.17, didn't include compressibility of the fluid therefore the flowrate spikes would be lower, thanks to fluid compression.

Unfortunately the values presented by the authors of publications [2,10,12] despite presenting the similar tendencies, are not the same. This may be the result of different assumptions and different research objects.

4 Conclusion

Using the methods shortly described above, it is possible to assess the leakage of the pump without building prototypes and conducting expensive laboratory tests. In most cases analytical models were prepared and verified using CFD simulations. The verification confirmed that the maximal error of the presented models does not exceed 20% and in most cases is even significantly lower.

Only the model of a gap between cylinder block and commutation plate proved to be too complex to reliably simplify it to mathematical equation. Therefore in the future it is planned to conduct a series of simulations, to build a bigger data base of results and make another attempt to analytically describe the flow through a gap between cylinder block and commutation plate.

It would be also advisable to conduct a series of laboratory test to verify models using experimental methods. Unfortunately it is very hard separate the sources of leakage from each other in working pump. Therefore the only reliable method is to measure the overall leakage and comparing it to the sum of leakage flow rates obtained from simulations or calculations.

5 Acknowledgments

The article includes the research introduced in PhD thesis [5] and continued in project funded by The National Centre for Research and Development within the framework of program LIDER:

Project no.: LIDER/22/0130/L-8/16/NCBR/2017

Project title: Hydro-mechanical automatic gearbox for agricultural vehicles and heavy machinery

Funding value: 1 197 500,00 PLN

References

1. Osiecki A. Hydrostatyczny napęd maszyn. WNT, Warszawa, 1998.
2. Złoto T. Modelowanie obciążenia hydrostatycznego i analiza zjawisk przepływowych w szczelinie rozrządu tarczowego pompy wielotłoczkowej osiowej. Politechnika Częstochowska, Częstochowa, 2007.
3. Osiecki, A. Osiecki L. Hydrstatic axial piston machine. European patent 0742870, 1999.
4. Patrosz P. Compensation of pressure peaks in variable displacement piston pump with cam driven commutation. Ph.D. Thesis, Gdansk, 2017
5. Chao, Q., Zhang, J., Xu, B. et al. Centrifugal effects on cavitation in the cylinder chambers for high-speed axial piston pumps. *Meccanica* 54, 815–829 (2019).
6. Jasiński R.: Influence of type of material on performance of hydraulic components in thermal shock conditions. *Solid State Phenomena*, Vol. 183, 2012.
7. Jasiński R.: Determination of ability of hydrotronic systems to start in low ambient temperatures. *Solid State Phenomena*, Vol. 164, 2010.
8. Z. Walczyk. Wytrzymałość materiałów-Teoria i przykłady Tom 2. Politechnika Gdańska, 1999.
9. Zastempowski. B. Badanie przepływu oleju przez dławik śrubowy. Ph.D. thesis, Gdansk University of Technology, Gdańsk, 1981.
10. Ivantysynova, M. Baker J. Power loss in the lubricating gap between cylinder block and valve plate of swash plate type axial piston machines. *International Journal of Fluid Power*, 10(2), 2009
11. Cho, J. Zhang, X. Manring, N.D. Nair, S.S. Dynamic Modelling and Parametric Studies of an Indexing Valve Plate Pump. *International Journal of Fluid Power*, 3(3), 2002
12. Wieczorek, U., & Ivantysynova, M. (2002). Computer aided optimization of bearing and sealing gaps in hydrostatic machines—the simulation tool caspar. *International Journal of Fluid Power*, 3(1), 7–20. <https://doi.org/10.1080/14399776.2002.10781124>
13. Pelosi, M., & Ivantysynova, M. (2009). A novel fluid-structure interaction model for lubricating gaps of piston machines. In *WIT Transactions on the Built Environment* (Vol. 105, pp. 13–24).
14. Ivantysynova, M., Huang, C. (2002). Investigation of the gap flow in displacement machines considering elastohydrodynamic effect. *Proceedings of the JFPS International Symposium on Fluid Power*, 2002(5–1), 219–229.
15. Hamrock, B. J. (1991). *Fundamentals Fluid Film Lubrication* of. Nasa Publication 1255.

